Green Chemistry

COMMUNICATION

View Article Online
View Journal | View Issue

Cite this: *Green Chem.*, 2019, **21**, 5521

Received 30th July 2019,
Accepted 13th September 2019

DOI: 10.1039/c9gc02676b

rsc.li/greenchem

Computational design of an intramolecular photocyclization reaction with state-selective reactivity: a strategy for indole synthesis†

Jingwei Zhou,[a] Lamei Li,[a] Ming Yan [b] and Wentao Wei *[a]

The development of a convenient and environmentally friendly indole synthesis method is of great methodological and pharmaceutical interest. In this work, we discovered an intramolecular photocyclization of carbonyls and tertiary amines for indole synthesis without relying on photocatalysts. A wide range of functional indoles were prepared with moderate to excellent yields under mild reaction conditions. Furthermore, our extensive quantum mechanics (QM) calculations and synthesis experiments revealed the 'state-selective reactivity' feature of this reaction, and different substrate types can achieve different yields through this feature. This new insight into the interplay between the 'state-selective reactivity' and the yields emphasizes its importance and gives guidance regarding the 'state-selective reactivity' for the high yield of various indole derivatives.

The indole nucleus is one of the most ubiquitous scaffolds and is abundant in natural products, pharmaceuticals and agrochemicals.[1] Thus, efficient and convenient indole synthesis methods are attracting increasing research attention. Over the past few decades, numerous methods have been developed.[2] Among them, visible-light-promoted synthesis of indoles offers a novel and efficient strategy under mild conditions.[3] Recently, Zhou[4] reported the application of visible light to generate α-amino alkyl radicals and the subsequent addition of alkynes to produce 3-acylindoles. The groups of Rueping[5] and Ye[6] independently reported the synthesis of indoles through the intramolecular addition of α-amino alkyl radicals to α,β-unsaturated carbonyl compounds under visible-light irradiation (Scheme 1a). Zhu and co-workers[7] developed an Ir-catalyzed synthesis method for indoles and other multi-substituted nitrogen heterocycles (Scheme 1b). Despite the convenience and effectiveness of photoredox catalysts, they are not without limitations, such as the concern about the need for expensive metals and ligands and the deactivation of catalysts. Besides economic deficiencies, even more important of the above approaches mediated by transition metals and other photocatalysts are the environmental deficiencies since many transition metals and photocatalysts are important contaminants and usually toxic. Therefore, there is an urgent need to develop new indole synthesis methods which are economic and environmentally friendly without losing convenience and effectiveness value. Excitingly, photochemistry triggered by ultraviolet light provides an acceptable practice to solve the above problem and has found widespread application.[8] Numerous photoinduced processes have been successfully initiated by using n → π* triplet-excited ketones, such as hydrogen abstraction,[9] photocyclization,[10] and Norrish reactions.[11] For example, ketone compounds whose electronic excitation involves the transition of a lone-pair electron from oxygen to the carbonyl carbon are inclined toward homolytic to diradical properties. Thus, the involved reactions depend on the innate properties of reactants without

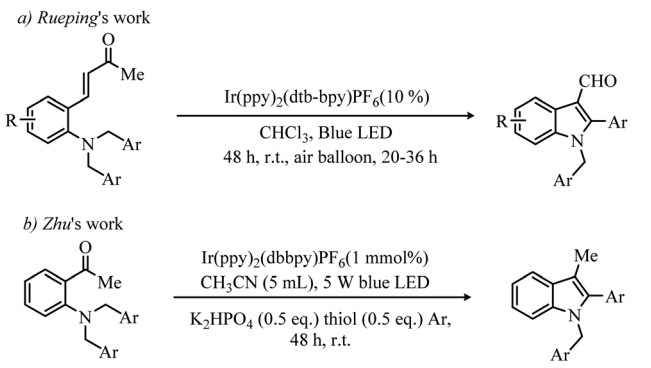

Scheme 1 Synthesis of indoles relying on the photocatalyst in previous studies: (a) Rueping's work (b) Zhu's work.

[a]*Institute of Clinical Pharmacology, Guangzhou University of Chinese Medicine, Guangzhou 510405, Guangdong, China. E-mail: wentao@gzucm.edu.cn*
[b]*Institute of Drug Synthesis and Pharmaceutical Process, School of Pharmaceutical Sciences, Sun Yat-sen University, Guangzhou 510006, Guangdong, China*

†Electronic supplementary information (ESI) available: Experimental procedures, computational method, references, Fig. S1–S12, Tables S1–S13, Scheme S1, characterization data, NMR spectra and molecular coordinates. See DOI: 10.1039/c9gc02676b

the assistance of photocatalysts. Obviously, photochemistry offers an opportunity for developing chemical reactions in a simple and costless way without affecting the environment, which is in accordance with the prospective environmental and techno-economic assessment system. Based on the above characteristic, remarkable work has been carried out by Li's team.[12]

Herein, inspired by the excellent characteristics and widespread application of photoinduced processes, we proposed a new method of indole synthesis without photocatalysts through the photocyclization of carbonyls and tertiary amines initiated by visible light (Scheme 2).

In our proposed scheme, we hypothesized a photocyclization mechanism involving a [1,6]-H shift reaction and a radical–radical coupling reaction. As shown in Scheme 2, triggered by light irradiation, our proposed substrates can be excited to undergo n → π* or π → π* transition from the ground state (S0) to form a singlet-excited ketone (first excited singlet state, S1) or a further triplet-excited ketone (first excited triplet state, T1) through intersystem crossing (ISC) from the S1 to T1 state. In the excited ketone, the excited single electron is distributed on the C1 and O1 atoms, forming the C1 radical and O1 radical, respectively. In the following step, an infrequent hydrogen abstraction of the [1,6]-H shift from the α-carbon (C2 atom) of the N1 atom to the O1 atom may occur to generate a C1–C2 diradical molecule (A or A′ state). Subsequently, the intramolecular C1–C2 radical coupling reaction of the diradical molecule can produce a stable intermediate (B state), which can continue to dehydrate and thus generate a more stable condensation product under the driving force of aromatization. Obviously, compared to direct dehydration, the addition of acid can accelerate the dehydration of the B state, forming the condensation product.

To verify the correctness of the proposed photocyclization reaction, before the synthesis validation, quantum mechanics (QM) calculations were used to simulate our proposed substrates. The detailed computational method is presented in the ESI.†

Our first task was to describe the reaction profile of the proposed photocyclization reaction. Four types of substrates, *i.e.*, tetrahydroisoquinoline derivatives, benzyl substituted 2-aminobenzophenone derivatives, tetrahydroisoquinoline-derived benzaldehydes, and alkyl amine substituted benzophenone derivatives, were considered. As shown in Fig. 1 and Tables S1 and S2,† all representative compounds (**1a**/**1j**/**1ae**/**1aj**) of the four types can react through the proposed [1,6]-H shift and radical–radical coupling mechanisms, ultimately forming the expected condensation products (**2a**/**2j**/**2ae**/**2aj**) through the dehydration mechanism. The resultant condensation product had lower free energy than the corresponding reactant, indicating that the photocyclization was thermodynamically favourable. In terms of kinetics, the low free energy barrier of the [1,6]-H shift reaction decided that the photocyclization can rapidly occur in a mild environment without the photocatalyst.

Furthermore, an intriguing 'state-selective reactivity' feature was found in the proposed photocyclization. For **1a** pertaining to **tetrahydroisoquinoline derivatives (Fig. 1a), once it jumped into the T1 state, it immediately enabled the [1,6]-H shift reaction with a 9.43 kcal mol^{-1} barrier to form the prospective C1–C2 diradical molecule (A state; Fig. S3 and S4†). The formed diradical molecule further underwent spin inversion after a small energy increase to generate a radical–radical coupling product (B state). The above reaction involved the participation of spin inversion (from triplet to singlet); accordingly, this spin-crossing phenomenon was termed 'two-state reactivity' (TSR).[13] A similar TSR was observed in **1j** from

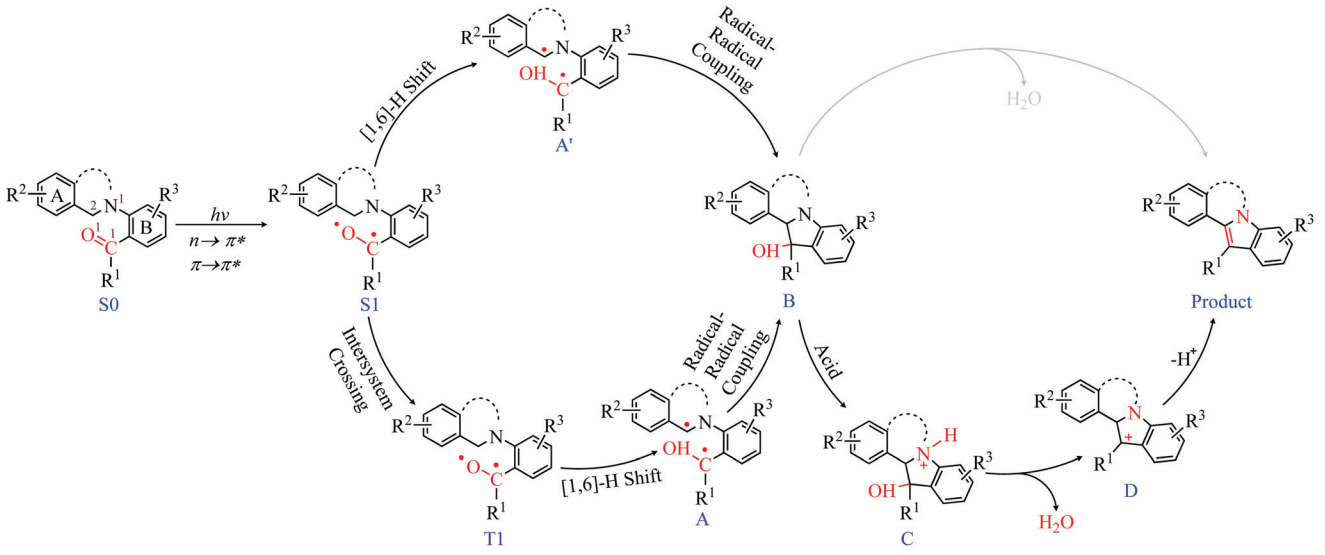

Scheme 2 Proposed photocyclization for the synthesis of indoles in this work. Our calculated UV absorption spectrum (Fig. S1†) and frontier molecular orbitals (Fig. S2†) of the optimized S0 state indicated a S0 → S1 transition corresponding to the n → π*/π → π* transition processes of HOMO → LUMO.

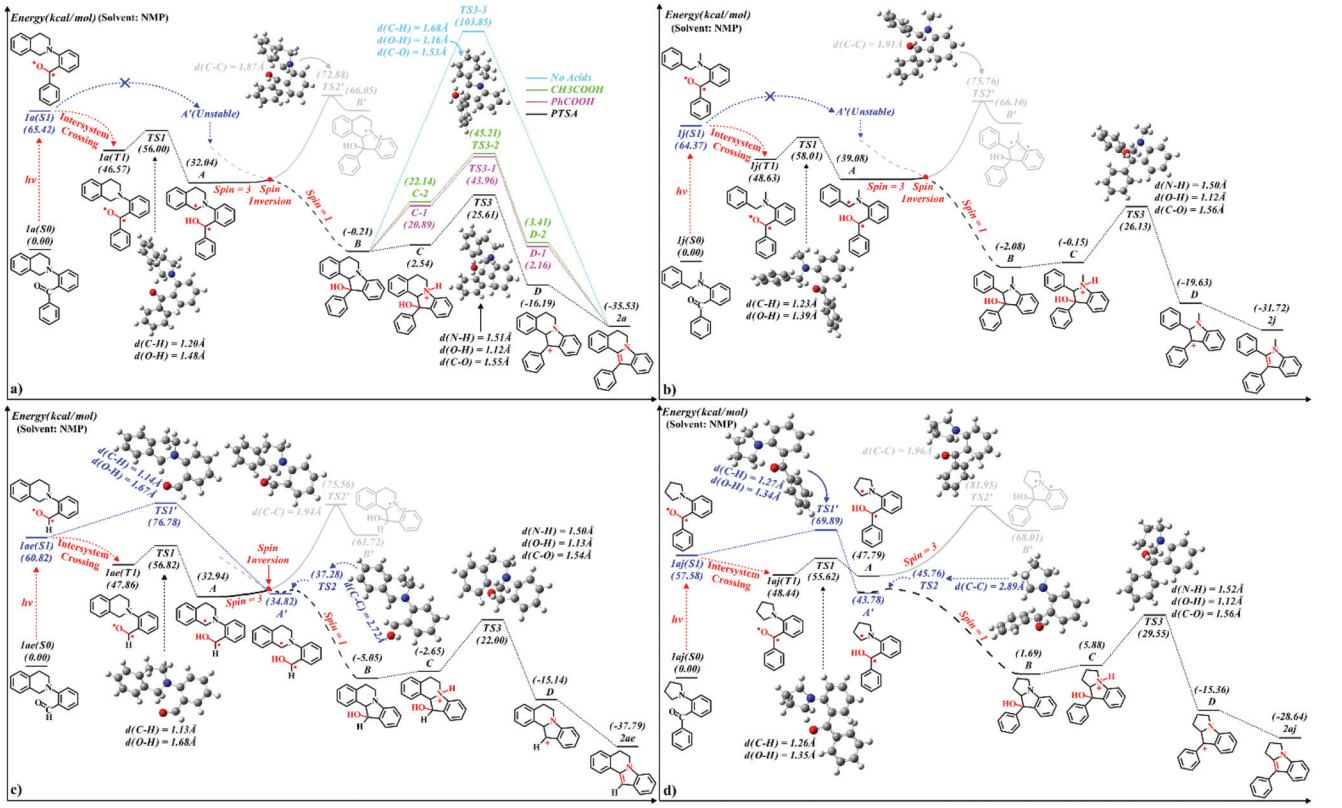

Fig. 1 Whole reaction profiles of the proposed photocyclization reaction for **1a** (a), **1j** (b), **1ae** (c), and **1aj** (d). Our computations were performed at B3LYP/6-31+G(d, p) in the PCM solvent continuum models (NMP). Besides the NMP solvent, other solvents (gas/toluene/THF/CH_2ClCH_2Cl/CH_3OH/CH_3CN/DMSO/water) were also considered (Fig. S10–S12 and Tables S6–S11†).

benzyl substituted 2-aminobenzophenone derivatives and in **1ae** assigned to tetrahydroisoquinoline-derived benzaldehydes (Fig. 1b and c), and their corresponding barriers of the [1,6]-H shift were 9.38 and 8.96 kcal mol^{-1}, respectively. However, TSR was not observed for **1aj**, which is an alkyl amine substituted benzophenone derivative (Fig. 1d). Although its T1 state can also go through the [1,6]-H shift with the lowest barrier of 7.18 kcal mol^{-1} to generate the diradical molecule, the non-existent intersection between the singlet potential energy surface (PES) and triplet PES determined that the diradical molecule cannot turn into the radical–radical coupling product through spin inversion; conversely, it can only climb over a high barrier (34.16 kcal mol^{-1}) to obtain another diradical molecule (B′ state) with high free energy. The nonsupport in thermodynamics and kinetics for the B′ state signified that photocyclization cannot occur depending on the T1 state. Then, the S1 state under compulsion replaced the T1 state to conduct the [1,6]-H shift reaction with a 12.31 kcal mol^{-1} barrier and produced a new diradical molecule (A′ state; Fig. S3 and S4†). The succeeding radical–radical coupling reaction of the A′ state overcame a very small barrier of 1.98 kcal mol^{-1}, and the presumptive radical–radical coupling product formed without spin inversion. Considering that photocyclization based on the S1 state proceeded on surfaces with uniform spin multiplicity, it was classified as 'single-state reactivity' (SSR).[13] A similar SSR was observed in **1ae** (Fig. 1c), and the corresponding barriers of the [1,6]-H shift and radical–radical coupling were 15.96 and 2.46 kcal mol^{-1}, respectively. This finding indicated that **1ae** has dual properties of TSR and SSR. Thus far, our computations confirmed that despite the similarity of these reactions to the photocyclization of carbonyls and tertiary amines, different substrate types had different state reactivities. Thus, we next attempted to identify the origin of 'state-selective reactivity'.

Considering that the 'state-selective reactivity' involved the S1 and T1 states, the ISC (S1 → T1) was first considered. As shown in Fig. 1, each of the ISC for **1a**/**1j**/**1ae**/**1aj** was thermodynamically favorable due to the lower free energy of its T1 state than that of its S1 state. However, their free energy gaps (Table 1 and Fig. S5a and b†) between the S1 and T1 states for **1a**/**1j**/**1ae**/**1aj** were −18.85, −15.74, −12.96, and −9.14 kcal mol^{-1}, respectively, demonstrating the strongest ISC spontaneity for **1a** and the weakest for **1aj**. The MOMAP package[14] was used to examine the kinetics of ISC. The calculated ISC rate constants (k_{ISC}) for **1a**/**1j**/**1ae**/**1aj** were 5.06×10^4, 4.35×10^4, 3.39×10^4, and 2.77×10^4 s^{-1}, respectively, indicating that the occurrence of ISC was most easy for **1a** and most difficult for **1aj** (Table 1 and Fig. S5c†). A stronger spontaneity meant more occurrence of the S1 state transferring to the T1 state, and a larger k_{ISC} meant quicker ISC. Therefore, considering the

Table 1 Thermodynamics and kinetics properties of ISC (S1 → T1) for **1a/1j/1ae/1aj/1al/1ao** (NMP solvent), and their single electron distribution of frontier molecular orbitals (SOMO-1/SOMO) for the S1 and T1 states. More molecules are shown in Table S4. N1, C1 and O1 atoms can be referred to from Scheme 2

	ISC (S1 → T1)		Single electron distribution (%)[c]				
			SOMO-1/SOMO(S1/T1)				
	Gap[a]	k_{ISC}[b]	N1	C1	O1	Total O1	R.[d]
1a	−18.85	5.06×10^4	19.51	11.46	10.44	11.48	TSR
			14.90	14.56	12.52		
			27.73	2.57	20.48	18.02	
			0.82	24.39	15.55		
1j	−15.74	4.35×10^4	18.82	11.38	9.05	11.65	
			16.66	17.60	14.25		
			31.73	3.32	23.35	19.13	
			0.90	14.32	14.91		
1ae	−12.96	3.39×10^4	41.94	7.25	13.65	16.17	TSR/SSR
			12.85	20.72	18.68		
			25.85	2.89	19.35	19.92	
			1.03	28.50	20.48		
1aj	−9.14	2.77×10^4	0.77	12.71	37.03	30.84	SSR
			1.98	21.44	24.64		
			31.95	3.55	28.22	21.73	
			1.64	24.06	15.23		
1al	−16.03	4.80×10^4	16.49	11.46	11.45	11.80	TSR
			13.30	15.13	12.15		
			15.89	2.29	17.38	17.93	
			0.20	25.26	18.47		
1ao	−8.84	6.13×10^3	20.84	10.59	9.40	11.71	—
			12.49	15.90	14.01		
			5.72	6.25	48.88	32.86	
			2.14	20.45	16.84		

[a] Gap, energy gap between S1 and T1 states, kcal mol^{-1}. [b] k_{ISC}, rate constant of ISC, s^{-1}. [c] For each molecule, from top to bottom are single electron distributions of SOMO-1 for the S1 state, SOMO for the S1 state, SOMO-1 for the T1 state and SOMO for the T1 state, respectively. [d] R., reactivity.

thermodynamics and kinetics, the most S1 state of **1a** quickly transferred to the T1 state, and second to fourth were the S1 states of **1j**, **1ae**, and **1aj**, respectively. As a result, **1a**/**1j**, **1aj** and **1ae** presented TSR, SSR, and dual reactivity, respectively.

The frontier molecular orbitals and their corresponding single electron distributions were subsequently analyzed. As shown in Table 1 and Table S3 and Fig. S2 and S5d–f,† the single electron generated by the HOMO → LUMO transition of the ground state (S0) was distributed on N1, C1, and O1 atoms in the S1 and T1 states. For the S1 state of **1a**, the single electron distribution probability on the O1 atom was 10.44% in the SOMO-1 orbital and 12.52% in the SOMO orbital. The corresponding data for the T1 state were 20.48% and 15.55%, respectively. Obviously, the total single electron distribution probability on the O1 atom for the T1 state was higher than that for the S1 state (18.02% *vs.* 11.48%). Similar phenomena were observed for **1j**, whose total distribution–probability ratios between the T1 and S1 states were 19.13% *vs.* 11.65%. More single electrons distributed on the O1 atom meant more ease in the hydrogen abstraction of the [1,6]-H shift reaction. Thus, **1a** and **1j** preferred to present TSR rather than SSR to some extent. Different from **1a** and **1j**, the total single electron distribution probability on the O1 atom for the S1 state of **1ae** increased to 16.17%. Although it was still lower than that for the T1 state (19.92%), the increase in probability apparently gave the S1 state a chance to realize the [1,6]-H shift with a high barrier (15.96 kcal mol^{-1}). This finding indicated the dual properties of **1ae**. Interestingly, the total single electron distribution probability on the O1 atom for the S1 state of **1aj** further increased to 30.84% which even exceeded that for the T1 state (21.73%). Thus, compared to **1ae**, a lower barrier of the [1,6]-H shift reaction (12.31 kcal mol^{-1}) emerged for the S1 state of **1aj**. Obviously, more SSR was observed for **1aj**. Combining the analyses of ISC and single electron distribution showed that from **1a** to **1aj**, the single electron distribution probabilities on the O1 atom for the S1 and T1 states gradually increased, leading to a gradual decrease in the barrier of the [1,6]-H shift reaction. Therefore, the photocyclization from the S1 state gradually became possible. Meanwhile, owing to the gradual increase in the difficulty of ISC, k_{ISC} even tended to be smaller than the reaction rate of the [1,6]-H shift from the S1

state, which may have led to the absence of an intersection for spin inversion. Consequently, photocyclization from the T1 state gradually became impossible despite the increased suitability for the [1,6]-H shift to proceed. Thus, although the reactions were similar to photocyclization, the different substrate types led to different state reactivities. The oscillator strength, SOMO orbital energy gap, and ESP charge were further analyzed to confirm the 'state-selective reactivity' (Fig. S5b and c, Fig. S6 and Table S3†).

During the above analysis processes, another phenomenon was observed, *i.e.*, under the same distribution probability on the O1 atom for the S1 state and T1 state, the T1 state may have been more suitable to undergo the [1,6]-H shift because of the lower barrier (Fig. S5f†). For example, the 11.48% and 11.65% distribution probabilities for the S1 states meant that **1a** and **1j** were not able to undergo the [1,6]-H shift, whereas the corresponding 18.02% and 19.13% for the T1 states were sufficient to decrease the barrier to 9.43 and 9.38 kcal mol^{-1}, respectively. Moreover, 16.17% for the S1 state of **1ae** provided 15.96 kcal mol^{-1} of the barrier, whereas 19.92% for the T1 state provided 8.96 kcal mol^{-1} of the barrier. Another example was **1aj**, which showed the corresponding values of 30.84% and 12.31 kcal mol^{-1} for the S1 state, and 21.73% and 7.18 kcal mol^{-1} for the T1 state. Accordingly, we proposed a hypothesis about the 'state-selective reactivity' that TSR molecules underwent photocyclization more quickly with an excellent yield, whereas SSR molecules had an inferior yield.

Considering the theoretical feasibility of our proposed photocyclization, our next task was to validate it and confirm its 'state-selective reactivity' through experiments. As shown in Scheme 3, under the optimum photocyclization conditions, we successfully obtained the expected products **2a**/**2j**/**2ae**/**2aj** from reactants **1a**/**1j**/**1ae**/**1aj**, respectively, indicating the feasibility of the proposed photocyclization for indole synthesis. Moreover, the 85% high yield of **1a** and the 56% low yield of **1aj** confirmed the proposed hypothesis about 'state-selective reactivity'. Besides **1a**/**1j**/**1ae**/**1aj**, we also expanded the derivatives of the four types. For tetrahydroisoquinoline derivatives (Scheme 3a), both substrates with functional groups substituted on the tetrahydroisoquinoline phenyl ring (**1b–1e**) and the substrates with functional groups substituted on the phenyl ring of the R^1 moiety (**1f–1i**) provided the products **2b–2i** with excellent yields, even as high as 91% (**1e**). For benzyl substituted 2-aminobenzophenone derivatives (Scheme 3b), except for the substitution on the N1 atom with phenyl groups (**1n**) that led to a high yield (83%), the same as that for tetrahydroisoquinoline derivatives, the remaining N1-substituted substrates (**1k–1m**) and the substitution substrates of R^2 and R^3 groups (**1o–1s**) contributed to the visibly lower yields than those for tetrahydroiso-

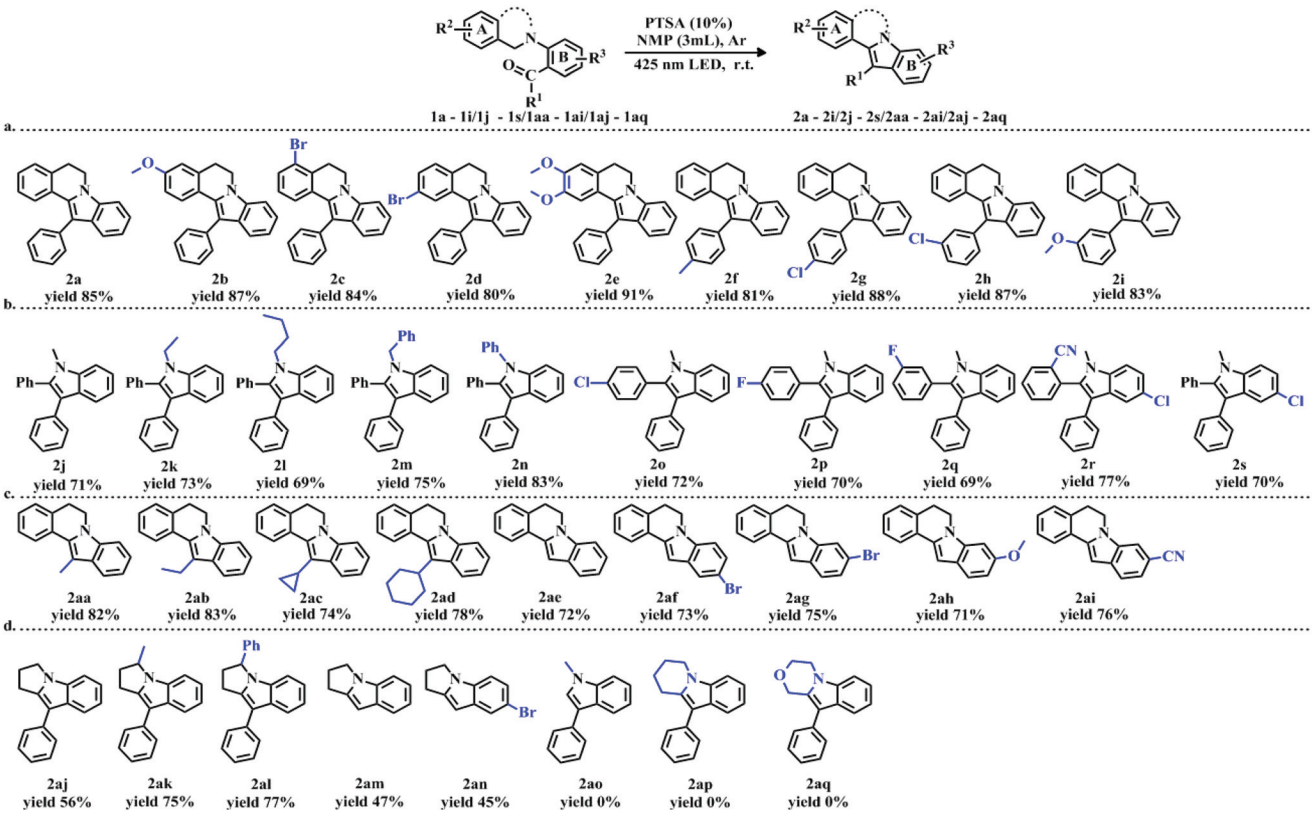

Scheme 3 Intramolecular photocyclization reaction of substrates: (a) substrates **1a–1i**, (b) substrates **1j–1s**, (c) substrates **1aa–1ai**, (d) substrates **1aj–1aq**. The reaction condition optimization is shown in Table S12.† Reaction conditions: Substrates **1a–1i/1j–1s/1aa–1ai/1aj–1aq** (0.3 mmol), NMP (3 mL), room temperature, 425 nm, 24 h, under an argon atmosphere, isolated yield. For **1aj–1aq**, the reaction time was prolonged to 72 h.

quinoline-derived benzaldehydes (Scheme 3c), the nonpolar-group-substituted substrates of the R^1 group (**1aa–1ad**) and the polar-group-substituted substrates of the R^3 group (**1af–1ai**) presented tolerable yields. These yields seemed to be lower than those of tetrahydroisoquinoline derivatives but were sufficient to be compared favorably with those of tetrahydroisoquinoline derivatives. For alkyl amine-substituted benzophenone derivatives (Scheme 3d), apart from the substrates with the substitution of methyl (**1ak**) and phenyl (**1al**) groups on the α-carbon of the N1 atom, which were in turn isolated in high yields of 75% and 77% of the expected products (**2ak** and **2al**), all remaining substituted substrates (**1am–1aq**) gave poor yields. Moreover, the *N*-methyl (**1ao**), -morpholine (**1ap**) and -piperidine (**1aq**)-substituted substrates did not even react at all, and the raw materials were recovered completely. The above experimental results showed that the yield of tetrahydroisoquinoline derivatives was obviously higher than that of benzyl-substituted 2-aminobenzophenone derivatives and tetrahydroisoquinoline-derived benzaldehydes, which further exceeded those of alkyl amine-substituted benzophenone derivatives. These results further confirmed our hypothesis about 'state-selective reactivity'.

Some of the abovementioned substrates were used to calculate and further confirm our hypothesis. For **1al**, which introduced a phenyl to **1aj**, the calculated energy gap between the S1 and T1 states was −16.03 kcal mol^{-1} and k_{ISC} was 4.80×10^4 s^{-1}, and the 17.93% single electron distribution for the T1 state and 11.80% for the S1 state indicated that the state reactivity of **1al** changed from SSR to TSR. Thus, a high yield of 77% was obtained based on the proposed hypothesis of 'state-selective reactivity'. The results reminded us that the substituent group could change the state reactivity of the photocyclization and to some extent could improve the yield of some extension substrates with SSR. For **1ao**, the low single electron distribution for the S1 state (11.71%) and the decrease in ISC in thermodynamics (−8.84 kcal mol^{-1}) and kinetics (6.13×10^3 s^{-1}) showed that neither TSR nor SSR was suitable for **1ao**, although its single electron distribution for the T1 state reached 32.86%. Thus, no reaction occurred. Other substrates (**1e**/**1i**/**1n**/**1ah**/**1ap**/**1aq**) were also analyzed from the ISC and single electron distribution (Fig. S7–S9 and Tables S4 and S5†), and all of them were consistent with the hypothesis about 'state-selective reactivity'. This finding confirmed the 'state-selective reactivity' of our proposed photocyclization.

Meanwhile, our proposed photocyclization reaction also presents another better characterization of competitiveness on the environmental aspect and sustainability compared to the previous conventional indole synthesis reaction. The detailed comparison is shown in Table S13.† Besides the competitiveness, the gram scale reaction was also employed to test the utility of our proposed photocyclization reaction. As shown in Scheme S1,† when compound **1a** was expanded to 5 mmol, accompanied by the load of PTSA decreased to 5%, an 80% yield of the desired product **2a** was isolated, which was almost as good as the 85% yield of the small sample experiment. It indicated the great potential applications of our proposed photocyclization reaction.

Conclusions

In summary, through extensive QM calculations and experimental verification, we proposed a clean and simple method of indole synthesis through the photocyclization of carbonyls and tertiary amines initiated by visible light without adding any photocatalyst. This method represents one of the examples that uses costless materials, low toxic solvents, and mild reaction conditions, shedding light on the development of green chemistry-oriented reactions. We further characterized the 'state-selective reactivity' of the photocyclization. Moreover, the 'state-selective reactivity' was correlated with the photocyclization yield and can be utilized to obtain high yields of indole derivatives.

Conflicts of interest

There are no conflicts to declare.

Acknowledgements

This work was supported by the National Science Foundation of China (21702236, 81803436 and 21772240) and the Doctor Initiated Project of Guangdong Natural Science Foundation (2016A030310459). We also thank the National Supercomputing Center in Guangzhou for providing the computational resources.

Notes and references

1 (*a*) E. Vitaku, D. T. Smith and J. T. Njardarson, *J. Med. Chem.*, 2014, **57**, 10257; (*b*) S. A. Patil, R. Patil and D. D. Miller, *Future Med. Chem.*, 2012, **4**, 2085; (*c*) S. Lal and T. J. Snape, *Curr. Med. Chem.*, 2012, **19**, 4828; (*d*) A. J. Kochanowska-Karamyan and M. T. Hamann, *Chem. Rev.*, 2010, **110**, 4489; (*e*) M. Bandini and A. Eichholzer, *Angew. Chem., Int. Ed.*, 2009, **48**, 9608; (*f*) P. Ertl, S. Jelfs, J. Muehlbacher, A. Schuffenhauer and P. Selzer, *J. Med. Chem.*, 2006, **49**, 4568; (*g*) T. Kawasaki and K. Higuchi, *Nat. Prod. Rep.*, 2005, **22**, 761.

2 (*a*) J. T. Pan, R. M. Zhao, J. M. Guo, D. M. Ma, Y. Xia, Y. X. Gao, P. X. Xu and Y. F. Zhao, *Green Chem.*, 2019, **21**, 792; (*b*) R. Lai, X. H. Wu, S. Y. Lv, C. Zhang, M. Y. He, Y. C. Chen, Q. T. Wang, L. Hai and Y. Wu, *Chem. Commun.*, 2019, **55**, 4039; (*c*) B. Zhou, Z. Wu, D. Ma, X. M. Ji and Y. H. Zhang, *Org. Lett.*, 2018, **20**, 6640; (*d*) T. Yoshida and K. Mori, *Chem. Commun.*, 2018, **54**, 12686; (*e*) H. D. Xia, Y. D. Zhang, Y. H. Wang and C. Zhang, *Org. Lett.*, 2018, **20**, 4052; (*f*) R. Mancuso and R. Dalpozzo, *Catalysts*, 2018, **8**, 458; (*g*) J. H. Lv, B. L. Zhao, L. Liu, Y. Han, Y. Yuan and Z. Z. Shi, *Adv. Synth. Catal.*, 2018, **360**, 4054; (*h*) I. Kumar, R. Kumar and U. Sharma, *Synthesis*, 2018, **50**, 2655; (*i*) A. A. Festa, *Chem. Heterocycl. Compd.*, 2018, **54**, 22; (*j*) D. I. Bugaenko, A. A. Dubrovina, M. A. Yurovskaya and

A. V. Karchava, *Org. Lett.*, 2018, **20**, 7358; (*k*) A. Andries-Ulmer, C. Brunner, J. Rehbein and T. Gulder, *J. Am. Chem. Soc.*, 2018, **140**, 13034; (*l*) W. T. Wei, X. J. Dong, S. Z. Nie, Y. Y. Chen, X. J. Zhang and M. Yan, *Org. Lett.*, 2013, **15**, 6018; (*m*) Z. Z. Shi and F. Glorius, *Angew. Chem., Int. Ed.*, 2012, **51**, 9220; (*n*) G. R. Humphrey and J. T. Kuethe, *Chem. Rev.*, 2006, **106**, 2875; (*o*) S. Cacchi and G. Fabrizi, *Chem. Rev.*, 2005, **105**, 2873.

3 (*a*) Y. Y. Liu, X. Y. Yu, J. R. Chen, M. M. Qiao, X. T. Qi, D. Q. Shi and W. J. Xiao, *Angew. Chem., Int. Ed.*, 2017, **56**, 9527; (*b*) W. Q. Liu, T. Lei, Z. Q. Song, X. L. Yang, C. J. Wu, X. Jiang, B. Chen, C. H. Tung and L. Z. Wu, *Org. Lett.*, 2017, **19**, 3251; (*c*) I. Alimi, R. Remy and C. G. Bochet, *Eur. J. Org. Chem.*, 2017, 3197; (*d*) G. P. D. Silva, A. Ali, R. C. D. Silva, H. Jiang and M. W. Paixão, *Chem. Commun.*, 2015, **51**, 15110.

4 P. Zhang, T. B. Xiao, S. W. Xiong, X. C. Dong and L. Zhou, *Org. Lett.*, 2014, **16**, 3264.

5 S. Q. Zhu, A. Das, L. Bui, H. J. Zhou, D. P. Curran and M. Rueping, *J. Am. Chem. Soc.*, 2013, **135**, 1823.

6 X. Q. Yuan, X. X. Wu, S. P. Dong, J. B. Wu and J. X. Ye, *Org. Biomol. Chem.*, 2016, **14**, 7447.

7 W. P. Li, Y. Q. Duan, M. L. Zhang, J. Cheng and C. J. Zhu, *Chem. Commun.*, 2016, **52**, 7596.

8 (*a*) A. M. Mfuh, J. D. Doyle, B. Chhetri, H. D. Arman and O. V. Larionov, *J. Am. Chem. Soc.*, 2016, **138**, 2985; (*b*) C. J. Li, *Chem*, 2016, **1**, 423; (*c*) T. S. Ratani, S. Bachman, G. C. Fu and J. C. Peters, *J. Am. Chem. Soc.*, 2015, **137**, 13902; (*d*) W. B. Liu, L. Li and C. J. Li, *Nat. Commun.*, 2015, **6**, 6526; (*e*) L. Li, W. Liu, H. Zeng, X. Mu, G. Cosa, Z. Mi and C. J. Li, *J. Am. Chem. Soc.*, 2015, **137**, 8328; (*f*) Y. C. Tan, J. M. Munoz-Molina, G. C. Fu and J. C. Peters, *Chem. Sci.*, 2014, **5**, 2831; (*g*) H. Q. Do, S. Bachman, A. C. Bissember, J. C. Peters and G. C. Fu, *J. Am. Chem. Soc.*, 2014, **136**, 2162.

9 P. Singh, *J. Chem. Soc. C*, 1971, **4**, 714.

10 N. C. Yang and D. D. H. Yang, *J. Am. Chem. Soc.*, 1957, **80**, 656.

11 C. Chatgilialoglu, D. Crich, M. Komatsu and I. Ryu, *Chem. Rev.*, 1999, **99**, 1991.

12 (*a*) Q. L. Yao, W. B. Liu, P. Liu, L. J. Ren, X. H. Fang and C. J. Li, *Eur. J. Org. Chem.*, 2019, 2721; (*b*) W. B. Liu, P. Liu, L. Y. Lv and C. J. Li, *Angew. Chem., Int. Ed.*, 2018, **57**, 13499; (*c*) P. Liu, W. B. Liu and C. J. Li, *J. Am. Chem. Soc.*, 2017, **139**, 14315; (*d*) W. B. Liu, N. Chen, X. B. Yang, L. Li and C. J. Li, *Chem. Commun.*, 2016, **52**, 13120; (*e*) L. Li, X. Y. Mu, W. B. Liu, Y. C. Wang, Z. T. Mi and C. J. Li, *J. Am. Chem. Soc.*, 2016, **138**, 5809.

13 (*a*) D. Schroder, S. Shaik and H. Schwarz, *Acc. Chem. Res.*, 2000, **33**, 139; (*b*) S. Shaik, D. Danovich, A. Fiedler, D. Schroder and H. Schwarz, *Helv. Chim. Acta*, 1995, **78**, 1393; (*c*) M. A. Robb, F. Bernardi and M. Olivucci, *Pure Appl. Chem.*, 1995, **67**, 783.

14 (*a*) Q. Peng, Y. L. Niu, Q. H. Shi, X. Gao and Z. G. Shuai, *J. Chem. Theory Comput.*, 2013, **9**, 1132; (*b*) Q. Peng, Y. P. Yi, Z. G. Shuai and J. S. Shao, *J. Am. Chem. Soc.*, 2007, **129**, 9333; (*c*) Q. Peng, Y. P. Yi, Z. G. Shuai and J. S. Shao, *J. Chem. Phys.*, 2007, **126**, 114302.